

Article

Utilization of Geodetic Methods Results in Small Open-Pit Mine Conditions: A Case Study from Slovakia

Slavomir Labant ¹, Marcela Bindzarova Gergelova ¹, Zofia Kuzevicova ¹, Stefan Kuzevic ², Gabriel Fedorko ^{3,*} and Vierošlav Molnar ⁴

¹ Institute of Geodesy, Cartography and Geographical Information Systems/Faculty of Mining, Ecology, Process Control, and Geotechnology, Technical University in Kosice, Letna 9, 042 00 Kosice, Slovakia; slavomir.labant@tuke.sk (S.L.); marcela.bindzarova.gergelova@tuke.sk (M.B.G.); zofia.kuzevicova@tuke.sk (Z.K.)

² Institute of Earth Resources Ecology/Faculty of Mining, Ecology, Process Control, and Geotechnology, Technical University of Kosice, Letna 9, 042 00 Kosice, Slovakia; stefan.kuzevic@tuke.sk

³ Institute of Logistics and Transport/Faculty of Mining, Ecology, Process Control, and Geotechnology, Technical University of Kosice, Letna 9, 042 00 Kosice, Slovakia

⁴ Institute of Computer Aided Production Technologies/Faculty of Manufacturing Technologies, Technical University of Kosice, Sturova 31, 080 01 Presov, Slovakia; vierošlav.molnar@tuke.sk

* Correspondence: gabriel.fedorko@tuke.sk; Tel.: +421-55-602-3143

Received: 25 April 2020; Accepted: 25 May 2020; Published: 27 May 2020



Abstract: Mining, especially surface mining, has a significant impact on the upper part of the soil cover, including fauna and flora. The article deals with the use of geodetic methods to observe the mining process and its possible impact on the environment. The created model can be used to design the recovery and reclamation of open-pit mines after their closure and mining termination. For the modeling of an open-pit mine, 2151 points from two stages of geodetic measurements were used. Graphical presentations of the geodetic measurements were compared with data from aerial photogrammetry. The measurement and processing results were used to visualize the spatial changes in the open-pit mine, which are necessary to take measures related to the recovery of the landscape affected by mining. Based on the calculation, 145.266 m³ were extracted during the period under exploration. When calculating the average excavated volume per working day, it was found that 188 m³ = 500 tons = 0.5 kilotons per day were extracted between the monitored periods. When comparing the original surface and the generated model of the open-pit mine, it was found that the entire top of the rock massif was permanently removed in the total volume of 3,421,000 m³. To capture the impact of mining on the surrounding environment, multispectral images of Landsat 7 and 8 during the observed period. Focused attention was divided into two factors, land surface temperature, and vegetation condition. The results from the temperature maps show that the open-pit mine is becoming a heat island. Analysis of the vegetative state confirms the rapid change in the health of vegetation, resp. reduction of its condition in the area around the open-pit mine. The presented results show that the selected methods and procedures are applicable in the conditions of the small mining company in Slovakia.

Keywords: geodetic measurement; mining process; open-pit mine; 3D model; volume determination; land surface temperature; NDVI

1. Introduction

A country's mineral wealth is considered to be an important economic factor and is linked to the economy of the country. Mineral resources are non-renewable natural resources, their extraction,

and subsequent processing must take into account the scarcity of their occurrence, the level of mining technologies by the objectives of sustainable development. Slovakia has the protection of mineral resources also mentioned in national regulations such as. Art. 4 (1) of the Constitution of the Slovak Republic, Act no. 44/1988 Coll. on the Protection and Utilization of Mineral Wealth-Mining Act, strategic documents National Strategy for Sustainable Development of the Slovak Republic and Updating the Raw Material Policy of the Slovak Republic.

Mineral wealth within the meaning of the Mining Act is made up of deposits of reserved minerals. Under this Act, mineral resources are in the ownership of the Slovak Republic, which grants legal entities the right to mineral resources extraction. This authorization entails certain obligations for the organization, which arise from Act No. 44/1988 Coll. Mining Act (§ 10 Obligations of the Organization in the Use of Reserved Deposit) and the Decree of the Ministry of Economy of the Slovak Republic on Mine Surveying Documentation in Mining Activities and Certain Activities Performed in the Mining Method (Decree of the Ministry of Economy of the Slovak Republic No. 1/1993 of 20 July 1993). The mining company is obliged to continually monitor the current state of these deposits by keeping the mine surveying documentation on the condition and process of the mining as well as in terms of the number of reserves and their inventory and to minimize the adverse environmental impacts of mining. By creating predictive models for the diffusion of pollutants, it is possible to help reduce the adverse impacts of mining activities in open-pit mines [1]. The works and processes of surface mining can be divided into several phases, which are connected and create a so-called life cycle of open-pit mine (Figure 1). An important part of the first phase of the exploration is also the classification of inventories into economic reserves (can be extracted now) and potentially economic reserves (currently cannot be effectively extracted). In the second phase, the organization is obliged to draw up a plan to prevent, reduce, and eliminate environmental burdens resulting from the proposed extraction procedures and the method of opening the deposit. The Environmental Impact Assessment (EIA) procedure is also part of the mining proposal [2]. The third phase is the construction of the open-pit mine and workplaces related to mining activities. Mineral processing activities may also be included. The fourth phase is the actual extraction of the mineral and its possible mineral extraction and refinement. Overall, this phase may represent the longest period e.g., at the current mining level, the reserves of the raw material in the open-pit mine are sufficient for mining for 150 years. After mining termination by mineral deficiency or other adverse circumstances (reduced demand for raw materials, financial difficulties, etc.), the mine closure phase and reclamation of the disturbed natural environment follows.

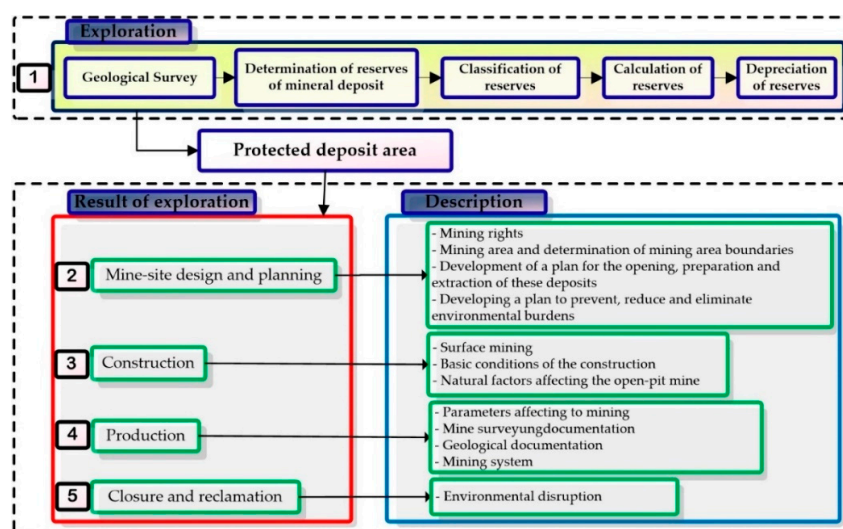


Figure 1. Life cycle of an open-pit mine (processed following the Slovak Republic mining legislation).

An Environmental Impact Assessment (EIA) is considered to be one of the main instruments of international environmental policy to promote sustainable development. The EIA covers all phases of the lifecycle of the extraction process. Slovakia has a database of all EIA proceedings on the environmental information channel (www.enviroportal.sk).

Mineral extraction, whether surface or underground, can have negative effects on the environment [3,4], human health [5] and often represents a major impact on the environment [6–8]. Many countries with a rich mining history often have to deal with the remnants of mining activities, which may constitute an environmental burden on the country and the population [9]. A solution such as burdens through reclamation [10] is time-consuming and costly.

The supervision of compliance with the Mining Act and related laws and regulations in the territory of the Slovak Republic is performed by the Main Mining Office based in Banská Štiavnica (<http://www.hbu.sk>) in cooperation with district mining offices. In 2018, it supervised entities using a total of 939 mineral deposits (566 reserved deposits and 373 non-reserved mineral deposits). One part of the yearly remittance from the mining area, royalty payments are transferred to the Environmental Fund (www.envirofond.sk). For the year 2018, the amount paid was € 2,316,820.99. The Fund was established to provide state support for environmental care and the creation of the environment on the principles of sustainable development. One of its tasks is to eliminate the consequences of mining activities and to secure or liquidate old mining works.

Documentation and visualization of the extraction area are closely connected with surface mining. The idea of documenting the geospatial distribution of an open-pit mine through the application of selected geodetic methods, technologies, and software is a way to constantly monitor spatial changes in mining operations. The timeliness of the concept of the solution of our study in the world, in the field of current research, is confirmed by the scientific work of the team of authors [11]. This work state to “*public institutions and host local communities also need access to high-quality spatial information to assess the benefits and risks of the decision-making process on sustainability issues in mining operations*”. Insufficient access to spatial information can lead to incorrect decisions, according to the cited article.

Also, in surveying, the requirements for accuracy of measuring, setting out and processing of geodetic data are increasing. The innovations of measurement technologies and processing software make geodetic work easier, whether they are collected, processed or analysed. One of the typical examples is geodetic surveying of the surface of the open-pit mine and subsequent determination of the extracted volume between two periods of time. Various measuring technologies and systems are used for geodetic measurement. If the terrain is accessible and the sky is clear, with expected benefits can be used the Global Navigation Satellite System (GNSS). GNSS is used to determine geodetic points, to measure the pit bottom and individual pit benches of the open-pit mine [12], for production planning [13], but also in monitoring the deformations and landslides resulting from the extraction of mineral resources [14]. If the surface is inaccessible, for collection of spatial information in open-pit mine is the most commonly used electronic tachymetry, terrestrial laser scanning [15,16], remote sensing (RS) [17] or oblique photogrammetry in particular by Unmanned Aerial Systems (UAS) [18–20].

GNSS are used to accurately determine location and time anytime, anywhere on Earth, regardless of the current weather conditions. The only condition of GNSS technology is the need for direct visibility to the sky. For geodetic measurements, using the location services, it makes it possible to accurately locate the open-pit mine and measure its available parts for the surveyor. The accuracy of the results of GNSS measurement can be significantly impaired due to: multipath, low elevation satellites, shadowing, unfavourable satellite distribution, ionosphere and troposphere effects, etc. The surveyor has to ensure that such degrading impacts do not affect the accuracy and reliability of the results. The most commonly used measurement methods are according to (<http://www.skpos.gku.sk/>; www.leica-geosystems.com; www.trimble.com):

- static method (not absolute positioning) that uses long observation (only among tens of minutes or a few hours) with accuracy in a horizontal position is $m_p = \pm 3 + 0.5 \cdot b$ ppm [mm] and in the vertical

position, it is $m_h = \pm 5 + 0.5 \cdot b$ ppm [mm] (where parameter b is the distance of the baseline measurement expressed in km),

- real-time network (RTN) relative positioning, where the rover has built-in software that instantly processes collected information from a permanent station and satellites. It is a relative positioning of points to the permanent station. The accuracy achieved in determining the horizontal position is $m_p = \pm 8 + 0.5 \cdot b$ ppm [mm] and in the vertical position, it is $m_h = \pm 15 + 0.5 \cdot b$ ppm [mm] (where parameter b is the distance between the rover and the reference station expressed in km).

Tachymetry with Total Station is a fast-geodetic measurement method in which the position and height of the points of the Earth's surface can be determined simultaneously [21]. At present, electro-optical tachymetry in combination with GNSS technology is used most frequently to determine the position of points in 3D space using the spatial polar method [22]. The use of TS to determine the position of points in 3D using the spatial polar method provides a high-quality set of geodetic measurements [21]. The typical accuracy of the measured horizontal ω and vertical z angle is usually $m_{\omega,z} = 0.0003^s = 1''$ in the present time. Selective data collection involves manual targeting on the reflection system by the measure of the points that characterize the course of the generalized terrain relief of the mapped area. In the present time, the typical accuracy of measured length with using a surveying prism is $m_s = 1 + 1.5 \cdot s$ ppm [mm], where s is slope distance. Non-selective data acquisition is the automatic measurement of surface points that form a square grid with a selected grid interval using a passive reflection system. The typical accuracy of measured length without using a surveying prism is $m_s = 2 + 2 \cdot s$ ppm [mm], where s is slope distance in the present time (www.leica-geosystems.com; www.trimble.com).

Terrestrial Laser Scanning (TLS) currently provides the most progressive and efficient way to collect large amounts of spatial data to create a digital 3D model. TLS is based on the acquisition of a high-density point cloud in a very short period using different techniques: pulse-based (time-of-flight) or phase-based. Most scanning systems determine the position of points by the spatial polar method. The scan result is a point cloud from which it is possible to create a very accurate 3D model of open-pit mine [16,23,24]. Currently, terrestrial scanners achieve 3D positional accuracy of 3 mm at 50 m or 6 mm at 100 m at a scanning speed of up to 1,000,000 points per second. Each point in the dataset contains the coordinates X, Y, Z, intensity I and colour shades R, G, B [25]. The colour shade is determined from the photo taken by the camera if it is built into the scanner.

Aerial photogrammetry (APhg) is mainly used for mapping the area, making numerical and graphical data for designing linear and areal constructions, and surveying the area carried out in the interest of environmental protection. Aerial survey images are obtained by special aircraft cameras. Recently, UAS have been used more to acquire geodata in smaller areas. Their advantage compared to satellite and aerial photogrammetry is their relatively low price (input and operating costs) and higher resolution. The main advantage is the flexibility in acquisition location which is not limited to a nadir view or views with identical angles. Significant limitations are their load capacity and range, greater load negatively affects battery life, relatively high sensitivity to meteorological conditions. Recently, UASs use GNSS real-time kinematic (RTK) or post-processing kinematic (PPK) technology to georeference images by assigning 3D coordinates and thus do not require the use of ground control points (GCP). With the latest processing photogrammetry software, we no longer need to know the characteristics of the camera and images [26,27]. Based on the processing of photogrammetric images it is possible to create a digital surface model (DSM) of open-pit mine [18].

Individual methods resp. technologies have their advantages but also disadvantages. For open-pit mine monitoring, it is still possible to use GNSS to determine geodetic points and consequently tachymetry with using the total station (TS). The combination of GNSS and TS still constitutes the basic and most common measurements for mapping and monitoring the open-pit mine. With the development of measurement techniques, GNSS + TS is still needed for the application of modern technologies, such as in terrestrial laser scanning [28–32], aerial photogrammetry using UAS [29,32,33], possibly also when comparing the results obtained from TLS and UAS [34,35].

When comparing the accuracy of point position using TS and TLS according to [28,31]: TS provides a more accurate point position, but there is uncertainty between the measured points and TLS provides a lower accuracy point position, but a denser point cloud. UAS and TLS are commonly used for 3D mapping, monitoring, and modeling of open-pit mines, including side slopes. If it is not possible to determine the GCP using the GNSS receiver, it is possible to use the TLS measurement with equally accurate results of the GCP localization [29]. A scientific study [30] compared different modern technologies used to geometry monitor of a deep open-pit mine with the conclusion. The TLS was able to record rock wall movement speed of 4 mm/h, TS from 25 mm/day. APhg can only be compared with TLS because it can provide to acquire a high-density point cloud for DTM modeling. The use of APhg provided more accurate results in the geometry determining of the rock walls in comparison with TS [33]. The combination of TLS and UAS was used to identify the main fault zones in the open-pit mine and to calculate the volume of the deposit reserves based on deep boreholes [34]. Volume calculate based on the use of UAS, where GCPs were determined using TLS (without the use of GNSS) provided results with a 1% difference in the total volume [35]. The management and economic aspect of the project solution are also important for the choice of used measuring methods and instruments [36].

The main idea of the scientific study is the application of geodetic methods to capture the current extent of mining in the open-pit mine. It is an overview of the used measurement technologies, implementation of geodetic measurements, processing of measured data (data), evaluation of the state of the spatial distribution of the quarry, and the intervention of mining into the landscape. The expected results of the study will create a 3D model of the open-pit mine as a result of surveying measurements carried out in two time periods, determine the volume of the extracted mineral. Mining in protected areas is also a problem in Slovakia, which focuses primarily on industrial materials (including limestone). The sites where these raw materials are located are ecologically important as they are mainly karst areas. The recommendation for the future is a thorough analysis of conflicts of interest, revision of forecasts, and reclassification of mineral reserves. The basis should be based on the mining boundary and strict adherence to the applicable regulations. The starting point could be a geodatabase containing mineral and protected area maps to assist in identifying potential conflicts in strategic planning for specific types of mining projects. To emphasize the environmental application, the scientific study provides a set of results of the evaluation of surface temperature and peak period of growth and development of vegetation of forest complexes based on the reflectivity of multispectral radiation in captured satellite images. The area was analysed using two indicators, namely land surface temperature and vegetation index (Normalized Difference Vegetation or NDVI). Concerning the main points of the study's direction, the study is dedicated to experts in the field of geodesy, geology, and environmental engineering.

2. Materials and Methods

2.1. Study Area

The Jaklovce mining area open-pit Kurtová skala mine is located in the Košice region, in the district of Gelnica, in the village of Jaklovce and the cadastral area of Jaklovce (Figure 2). The beginning of mining in the open-pit mine is in the 70–80 s. years of the 20th century. The study area is located in the northeast of the Slovak Ore Mountains in the Volovec Mountains. The solid deposit is located at an altitude of 710–753 m above sea level in the Baltic Vertical Datum-After Adjustment (BVDA) and is oriented to the southwest. Access to the open-pit mine is 5 km along an asphalt road from the beginning of the village Margecany.

The deposit of Jaklovce-Kurtova skala is classified as a deposit of non-reserved mineral and is formed by high purity limestone (content $\text{CaCO}_3 > 97\%$) [37]. The main extractive component of the deposit is calcium carbonate (CaCO_3), the extraction of which is shown in Figure 3.

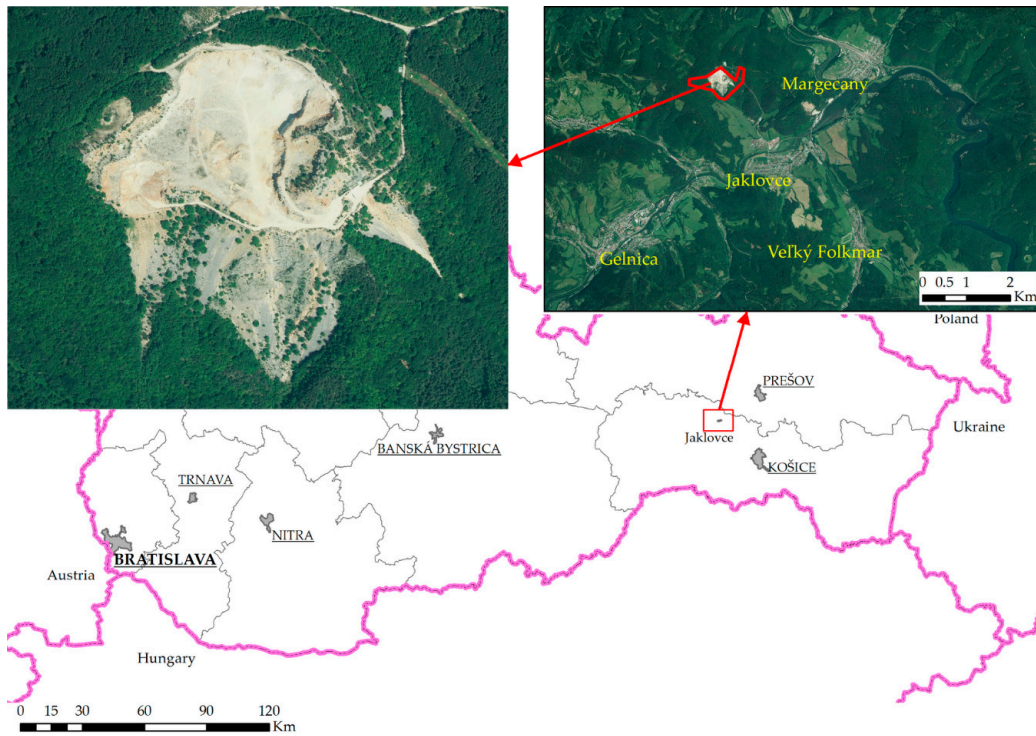


Figure 2. Study area of the open-pit mine.



Figure 3. Views of the pit benches in the open-pit mine. (a) Eastern view to the open-pit mine; (b) Northeast view from the pit bottom.

Limestone is often found in deposits with dolomite and subsequently, the rock is classified as dolomite limestone. High purity limestone has a wide range of applications in the metallurgical, chemical, rubber, food, glass, ceramic, and building industry. The annual mining production of limestone deposit Jaklovce over the last 9 years is shown in Figure 4.

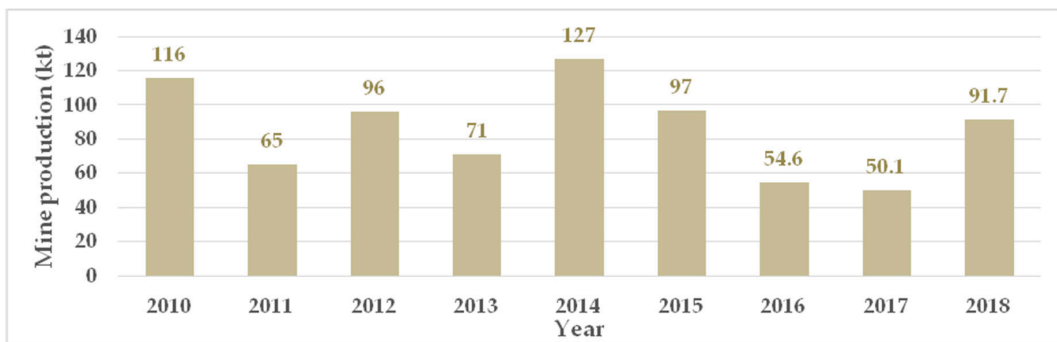


Figure 4. The high purity limestone extraction 2010–2018 in kilotons (kt).

2.2. Measurement Methods

In further fulfilment of the main idea of this study, several measuring and processing approaches were applied in the subject open-pit mine. The process of preparation, measurement, processing, and creation of the 3D model is illustrated as the diagrams (Figure 5). The result is the determination of the volume from the difference between the two surfaces. It is a sequence of steps applied to open-pit mine for the needs of further analyses. A GPS900CS GNSS receiver and a Viva TS15 I robotized universal measuring station (Leica, Heerbrugg, Switzerland) were used to measure in the open-pit mine. The accuracy of the positioning of the measured geodetic points using the RTK method at a position is max 10 to 15 mm and at height is max 20 to 30 mm. RTN measurement would be greatly accelerated if the GNSS receiver had a built-in tilt compensator. These receivers with tilt compensators are currently available on the market. When using TS, the measurement accuracy of horizontal and vertical angles, as well as the measurement accuracy of the length, are identical to the standard accuracy given in the Introduction at TS. When measuring using an optical prism, the maximum distance is 3500 m and the PinPoint non-prism measurement has a range of up to 1000 m (www.geotech.sk).

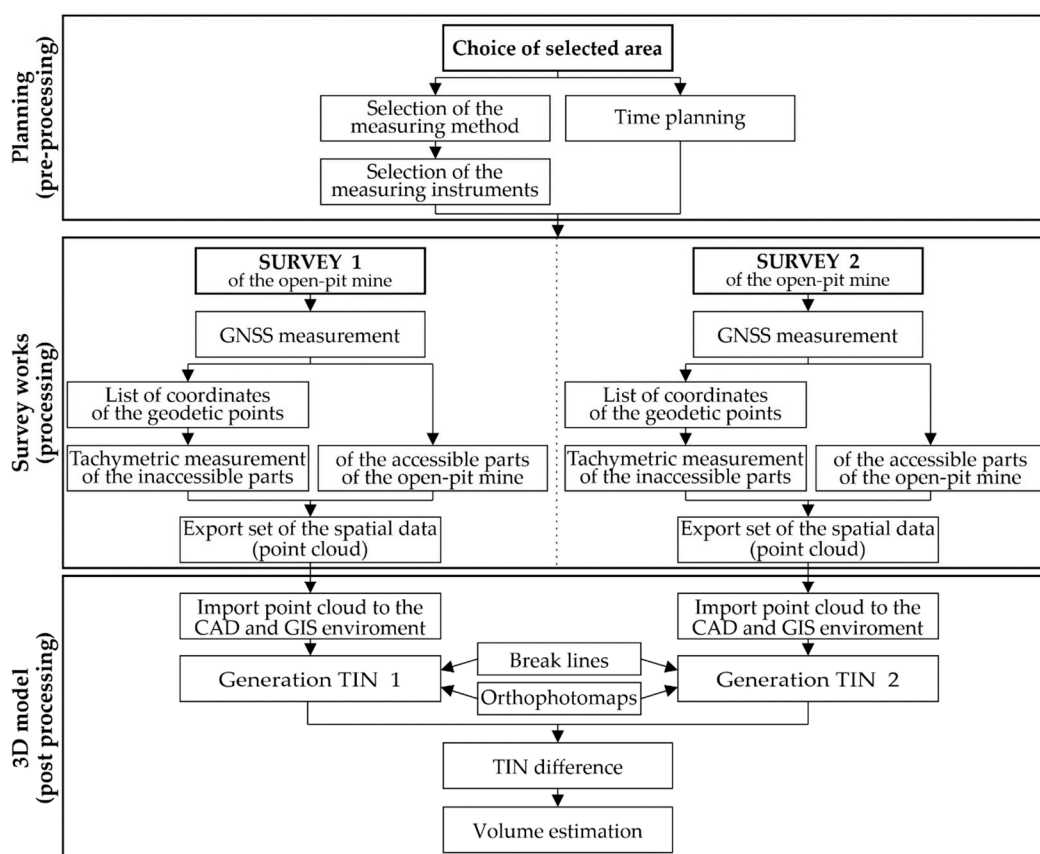


Figure 5. Workflow for the creation of the 3D model in the study area.

A measurement combination with a GNSS receiver and a total station was used, which briefly consists of the following steps (Figure 5 Survey works). The GNSS receiver (which needs the Internet to receive corrections) is used to determine the coordinates of the geodetic points. Subsequently, the measured coordinates are entered into a new job in the TS. When the TS is ready, the inaccessible parts of the open-pit mine can be started using measurement without a prism. After completing the measurement, it is necessary to export the measured data to a USB stick or SD card.

Other useful measurement technologies are TLS and APhg, which are currently the standards for large geodetic firms. For small geodetic firms, it is financially unavailable to extend the instrumentation with the mentioned types of measuring technologies (TLS and APhg). These measurement technologies

provide an unparalleled faster collection of spatial information, a higher density of points, shorten measurement time. But they require higher hardware performance for the software processing of the cloud point. For precise placement of measuring works using TLS or APhg, it is necessary to use GNSS resp. in combination with use with TS. TLS needs geodetic points with known coordinates and APhg needs GCP with known coordinates.

The available APhg results were used to compare the results of the TS and GNSS measurements. The flying period coincides with the monitoring period of the open-pit mine. The cloud points generated from aerial images were obtained from a commercial source. Data was created by photogrammetric processing of aerial stereo images and subsequent semi-automatic removal of vegetation and other objects created by human activity. The point cloud (X, Y, h) forms a square grid with a size of 2 m. In Table 1 are given further specifications of the commercially provided DTM.

Table 1. Basic parameters DTM from aerial photogrammetry (adapted from geodatastore.sk/katalog/digitalny-model-terenu).

Specification	DTM		
Coordinate system, realization	Uniform Trigonometric Cadastral Network (UTCN); UTCN03		
Vertical Datum	Baltic Vertical Datum-After Adjustment (BVDA)		
Vertical accuracy-RMSEh	0.3 m		
Point cloud	X, Y, h [m]		
Arrangement point cloud	Square grid		
Resolution—grid size	0.5 m	Resolution—grid size	2.0 m
Coverage of SR	Capital city—Bratislava	Regional cities	The rest of the Slovakia

RMSEh—Root Mean Squared Error of height.

A summary comparison of GNSS, TS, TLS, and APhg technologies is given in Table 2.

Table 2. Comparison of measuring technologies GNSS, TS, TLS, APhg.

Comparison Parameters	Compared Measuring Technologies			
	GNSS, RTK	TS	TLS	APhg
Price of the new instrument	≥5000 €	≥10,000 €	≥30,000 €	≥300,000 €
Usability level	basic	basic	higher	higher
Point determination accuracy	≥20 mm (3D)	≥1.5 mm (3D)	≥3 mm (3D)	≥50 mm (3D)
Point measurement speed	≤5 pt./min	≤5 pt./min	≤50,000 pt./s	≤20 photo/min
Average points	1–500	1–1000	1–100 Mio.	1–100 Mio.
Number of points on the area	≤250	≤250	≤20 Mio.	≤20 Mio.
Average distance from the area	0–2 m	5–100 m	5–100 m	100–2000 m (height)
Average distance of points	≤5 m	≤5 m	≥0.01 m	≥0.1 m
Duration of measurement	3 h	4 h	1.5 h	1.5 h
3D model processing	1 h	1 h	2 h	4 h
Hardware demands of PC	low	low	high	high

pt.—point; Mio.—Millions.

2.3. Measurement and Processing

In the open-pit mine, pit bottom, pit benches, and rocks walls were measured for volume determination between the two periods of measurement. The difference between the measurement periods is 1414 days, during which a certain volume was extracted. During the reconnaissance of the area of interest, the geodetic points were appropriately designed as well as a suitable measurement procedure. The measurement works were performed by the principles of generalization. It was important to measure of the characteristic points of ridgelines and breaklines of the open-pit mine. During surveying work, the rules concerning health and safety at work must be observed.

The measurement procedure was the same in both periods (Table 3). As usual before the terrestrial measurement with TS, it is necessary to enter into the instrument: atmospheric corrections (pressure,

temperature, and humidity of the air, eventually altitude), list of geodetic point coordinates from GNSS receiver (X, Y, h), and type of prism used or measurement without a prism.

Table 3. Two periods of surveying work using GNSS + TS.

Comparison Parameters	1st Period	2nd Period
Weather conditions	favourable	cloudy, then cleared
Surveyors	3	3
Geodetic points using Leica GPS900CS	5	5
Terrain points using Leica GPS900CS	87	103
Terrain points using Leica Viva TS15I	939	1022

Surveying works in the open-pit mine from the second period are shown in Figure 6. The location of the terrain points from the second period is shown in Figure 7. The blue circle shows points from TS and the red circle shows points from GNSS. A total of 1961 points measured on the Leica Viva TS15I total station and 190 points measured on the Leica GPS900CS GNSS receiver were used to create two open-pit mine models and to calculate the extracted volume of dolomite limestone.



Figure 6. Used instruments for measurement of the open-pit mine.

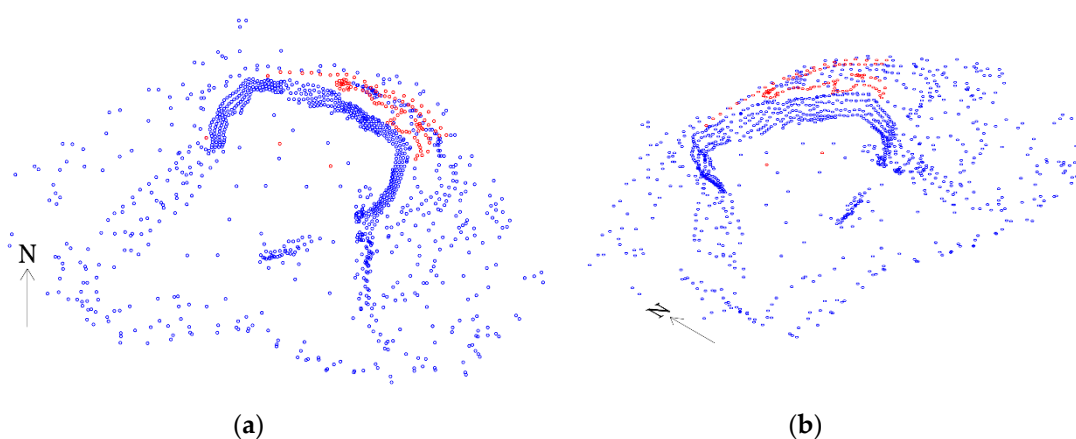


Figure 7. Two views of terrain points of the open-pit mine from the second survey period: by TS—blue circle, by GNSS receiver—red circle. (a) View from above; (b) Isometric view.

The data measured from the Leica GPS900CS GNSS receiver was processed in LeicaGeoOffice and then exported to a text file. Measured data were also exported to text files from TS Leica Viva TS15I. Text files of *.txt format contained point numbers, their coordinates in the coordinate system Uniform Trigonometric Cadastral Network (UTCN), and the heights in the BVDaA. The measured points from the two measurement periods of the open-pit mine were imported into the Microstation V8i with the Terramodeler superstructure as two terrains. Another 3rd terrain was created from the coordinates

of the point cloud generated from the processing of aerial images. All three terrains were imported as points of breaklines and terrain points. Subsequently, the processing and analysis of digital terrain models began.

2.4. Calculation of Normalized Difference Vegetation and Land Surface Temperature

For highlighting the environmental application, the scientific study analysed the spatial changes data in the open-pit mine using satellite imagery for the area shown in Figure 13. Specifically, these were the multispectral images from observations of the Landsat 8 and Landsat 7 satellites (Landsat-7, Landsat-8 image courtesy of the U.S. Geological Survey, Reston, VA, USA). Landsat images are an available and high-quality source of remote sensing data. The images were selected for June, where vegetation is assumed and with minimal cloud cover (less than 10%). For status display of the vegetation was chosen 2012, 2015, and 2019. The panchromatic image has at 15m spatial resolution and the multispectral image has 30 m. For our further analyses were chosen multispectral images.

The work [38] is devoted to the estimation of surface temperature in areas where surface mining takes place. The analysis of multispectral images from the reflectivity of the colour spectrum from the Landsat images for the monitoring of vegetation changes is dealt with in [39] and in the field of surface mining [40].

The temperature was calculated according to the USGS methodology [41,42] and the algorithm in the study by Avdan and Jovanovska [43]. For Landsat 8 images, band 10 was used for temperature calculation and Bands 4 and 5 for the NDVI index. For Landsat 7, Band 6 for temperature calculation and Bands 3 and 4.

3. Results and Discussion

To assess the state of the spatial distribution of the open-pit mine and the impact of mining into the landscape, a 3D model of the open-pit mine was created using CAD and GIS systems. DTM provided possibilities for modeling, analysing, and displaying terrain-related and topography-related phenomena [44], as well as follow geomorphological features at the level of a variety of processes occurring on the Earth's surface [45,46]. DTM is used in several scientific works as a basis for capturing specific changes caused by surface mining [47]. DTM also contents several analytical, visualization approaches supporting the creation of 3D models and mining objects [48].

To calculate the volume, it is necessary to create a DTMs from the available point clouds. These can be visualized using TIN, and GRID model or contour lines. Inserting breaklines does not affect the placement of terrain points, but changes the way the triangles are joined, increasing the accuracy of the volume calculation of the 3D irregular solids. The volume calculation can be performed on the whole area or only on a certain part. The accuracy and time of the calculation depend on the size of the grid. The basic procedure in software volume calculation according to [12]:

- (1) Creation of the 3D drawing (*.dgn).
- (2) Creating at least two terrains (DTM) by importing coordinate lists.
- (3) Visualization individual of the models, their checking and editing of triangles using breaklines.
- (4) Calculate the volume of an irregular body between two surfaces/terrains.

The volume of 3D solid is determined more precisely if [12]:

- The method of measurement and measuring instruments chosen are more accurate,
- a greater number of points are suitably morphologically distributed on the 3D solid,
- the surface of the 3D solid is more geometric,
- the more appropriate mathematical relationship is the approximated surface of the 3D solid,
- there is a greater number of elementary solid on which the 3D solid is broken down as a result of geometry.

3.1. Visualisation of the Geodetic Measurement in the Open-Pit Mine

On the modeling of open-pit mine was used 2151 points from two periods of geodetic measurements. Two DTMs were generated from the two measurement periods. Two DTMs were used to determine the extracted volume of dolomite limestone between the measured periods. Unrealistically generated parts of the contour models of the open-pit mine from the two periods were modified using breaklines. Before the volume calculation, a comparison of contour models from GNSS + TS vs. APPhg (the year 2015) was performed in the following section.

The visualization of the contour model from the measured data of the second period and the contour model from the points generated from aerial photogrammetry were compared. Based on a graphical comparison of the rock wall of the lower pit benches, it was found that aerial photogrammetry was performed before the terrestrial survey of the open-pit mine (Figure 8). A graphical comparison of rock wall models is shown on an orthophoto map. The rock wall in the open-pit mine can be divided into two zones. The first is the zone of the rock wall unaffected by mining. It is shown in black as an area of identical graphics. The second is the zone of the rock wall affected by mining. It is shown in green as an area of non-compliant graphics. The identical area is shown with minimal differences in position and height. Transverse profiles of the rock wall with marked 1, 3, and 6 are shown from these areas. The results of aerial photogrammetry confirm the correct location of the rock wall in the open-pit mine. Non-compliant areas of the rock wall marked in green colour are already affected by mining. Graphic representations show large differences in the location and height ratios of the rock walls of the pit bottom. In the green areas, it is possible to observe the moving forward of mining on the analysed rock wall. Provides evidence of this are shown the cross-sections marked with the numbers 2, 4 and 5.

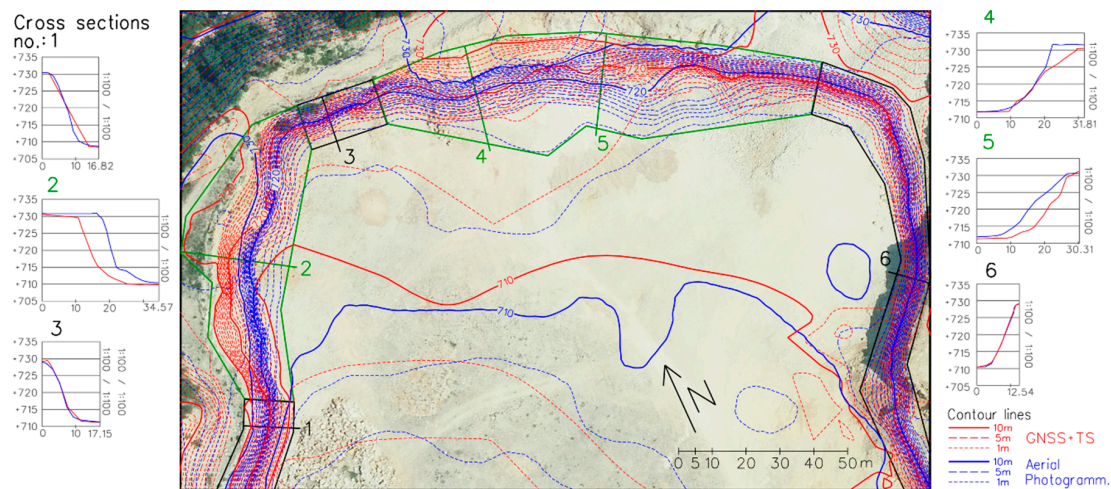


Figure 8. Graphical visualization of the contours of the rock wall of the pit bottom of the open-pit mine from the data of aerial photogrammetry and tachymetric measurement of the total station.

Based on the volume calculation, it was found that $145,266 \text{ m}^3$ were extracted in almost 4 years. A comparison of the changes in the mining process between the 1st (green contour lines) and 2nd (orange contour lines) periods are shown in Figure 9a. There were 1414 days between the measurement periods, of which 804 were working days. The average extraction per working day was calculated to be approximately 188 m^3 . This volume corresponds to approximately $500 \text{ t} = 0.5 \text{ kt}$ /working day at a density of dolomite limestone of 2.65 t/m^3 . The extracted weight of the limestone is 378.4 kt between two periods (according to Figure 4). The weight of the extracted limestone of 378.4 kt corresponds to the volume of $142,774 \text{ m}^3$ at a limestone density of 2.65 t/m^3 . The volume difference from the two sources is 2500 m^3 , which represents about 1.7% of the total volume. The differences in results can be caused by a generalization of the terrain in geodetic measurement and DTM processing. Even irregular

extraction during the year affects the total volume from Figure 4 converted to the number of working days per year.

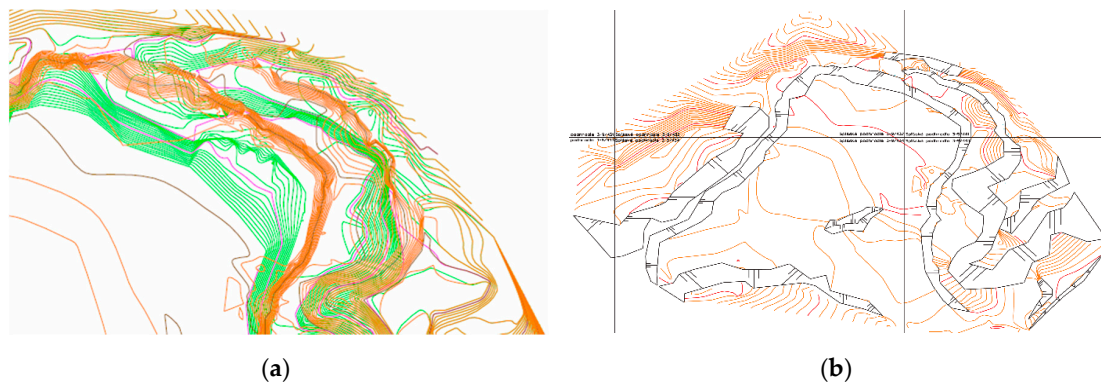


Figure 9. Graphical representation of the extraction process between two periods from GNSS + TS data and the representation of the technical hachures with the contour lines (1 m interval). (a) green—day 1; brown—1414. day of observation; (b) status at 1414. day of observation.

The contour lines are too dense on the rock walls in the mine map and are replaced by technical hachures in the direction of slope (Figure 9b). The current model from the second geodetic survey period (1125 points) was used for further visualization. By digitizing the mining map at a scale of 1:1000 from a previous measurement, 1020 terrain points were obtained from the surroundings of the open-pit mine. These points were used to create a complete 3D model of the open-pit mine with its surroundings. It is possible to create a triangular TIN model with the application of the colour type of territory type (Figure 10, upper DTM).

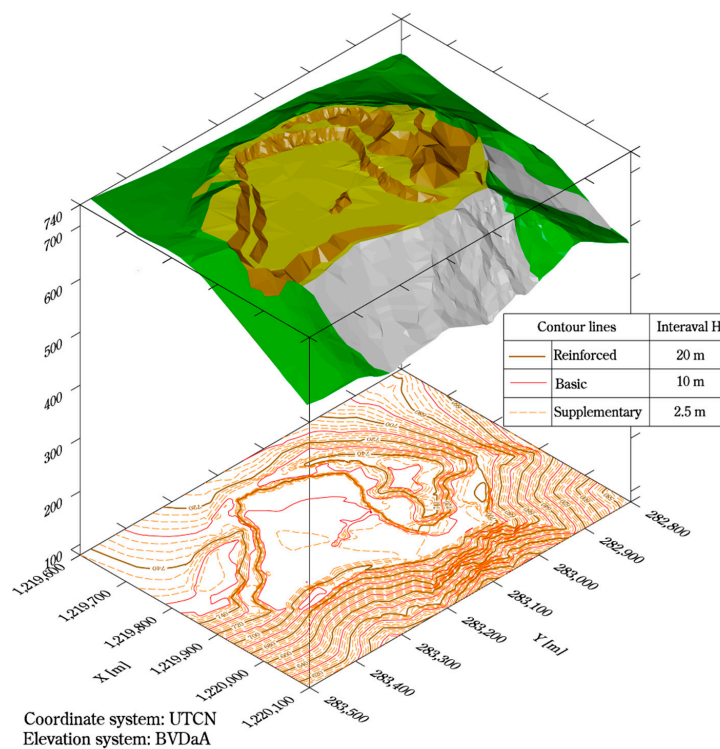


Figure 10. Graphical representation of the contour and TIN model of the open-pit mine with the application of colour resolution of the territory type.

The colour scale used distinguishes parts of the open-pit mine including its surroundings: available areas of individual pit benches—yellow; rock walls—brown; surrounding forest—green; embankments created by mining—grey. The contour model consists of isohypes (contour lines) with corresponding height data too. Contour lines are divided into basic contour lines (with an interval of 10 m), reinforced contour lines (with an interval of 20 m) and supplementary contour lines (auxiliary—with an interval of 2.5 m) (Figure 10, lower DTM).

To compare and show the impact of surface mining on the surrounding environment, a 3D surface model was created from contour lines from the topographic map background (Figure 11a). The topographic map shows the state of the surface before the area is affected by mining. The highest point of rock massif was at level 791 m. At the time of surveying, the highest working pit bench of the open-pit mine was at the level 753 m and the pit bottom of open-pit mine was at level 710 m. The spatial model is shown in Figure 11b was created in ArcGIS Pro from geodetic measurements and orthophoto was added for better visualization.

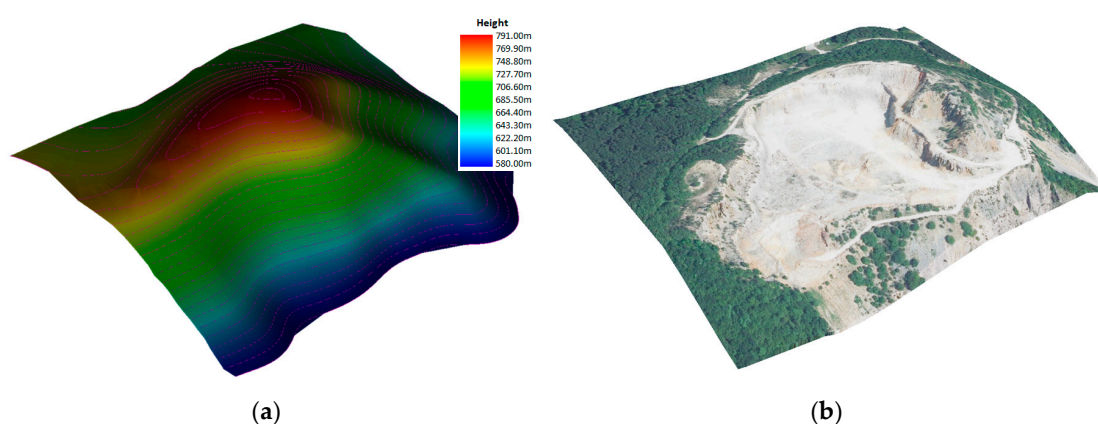


Figure 11. Comparison of visualization of two created models of the open-pit mine. (a) Model from topographic map (year 1980); (b) Model from geodetic measurement with orthophoto (present time).

A comparative model was created to capture spatial changes in the mining process and to impact the natural environment. The contour model of the original terrain from the period before 1980, i.e., before the beginning of mining (Figure 12), was imported into Google Earth. The contour lines model shows the original state of the surface for the reason of visibility and comparability with the current state. The calculation determined that the deposit had a volume loss of 3,421,000 m³ by the extraction of the entire top of the rock massif.

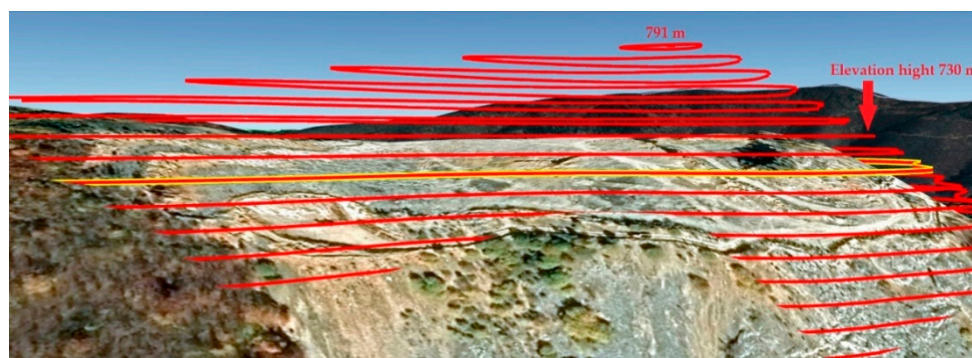


Figure 12. Graphical representation of rock mass loss (adapted from Google Earth, earth.google.com/web/).

In terms of subsequent and possible reclamation, the situation seems to be quite complicated. In the study area, the entire upper part of the rock massif was permanently removed. Given the service

life of the deposit of about 150 years, it is assumed that the entire rock massif can be gradually removed. Removal of the rock massif causes to permanent disruption of the natural environment (limestone rock was the habitat of rare plant species), and especially the microclimate of the region. It is essential that the basic climatological characteristics of the site, such as temperature and wind, be monitored since the removal of the obstacle could alter the airflow. The severity of the damage is assessed on a case-by-case basis and depends on the rarity and vulnerability of the affected habitats. If endemic sites are present in the site, the survival of the entire plant or animal population may be at risk.

In Figure 13 shows the area of the open-pit mine Kurtová skala, in the neighbourhood of which there is a protected bird area. To show the relative positions of the open-pit mine and bird area was selected area with dimensions of 4 km × 4 km (16 km²) close in the open-pit mine that was used for the processing and analysis of multispectral satellite images. Ongoing mining, especially blasting, can harm the bird population.



Figure 13. The relative position of the protected bird area and open-pit mine Kurt rock.

The minimum air distance between the mining area boundary and the protected area of the SKCHVU036 bird area is approximately 70 m and the distance from the queue is approximately 300 m. The transport itself after blasting operations (loading and unloading) is realized using high-volume mechanized wheeled transport, represented by loaders and trucks. The movement of equipment and vehicles, as well as the presence of humans, can negatively affect some species of birds. Part of the production technology is also the primary crushing of aggregates, which is another source of long-term noise of lower intensity, vibration, and dustiness.

Changes and severity of damage to the landscape structure can be monitored by analysis of aerial images (for smaller areas) or satellite images (larger areas). An overview of changes in the spatial distribution of the open-pit mine for the observed period is presented in Figure 14. Over the last 60 years since the beginning of mining (Figure 14a) the growing devastation of the original forest cover is visible (Figure 14b,c).

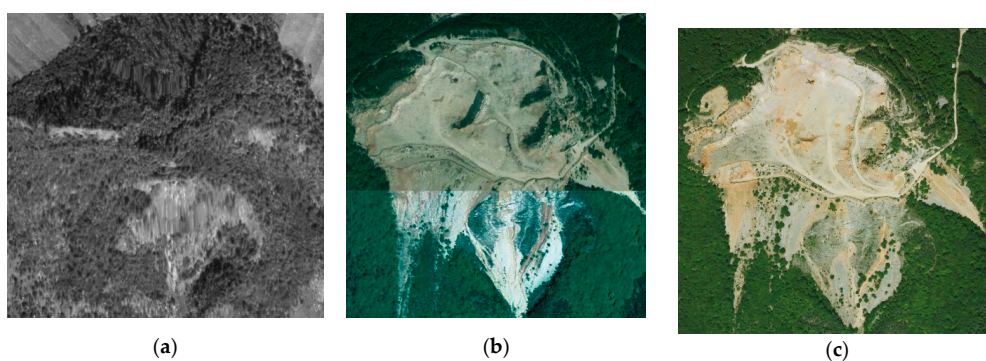


Figure 14. Spatial changes of the mineral deposit in time (Adapted from mapy.tuzvo.sk/HOFM/). (a) year 1950; (b) year 2000; (c) year 2017.

3.2. The Spatial Changes in Vegetation Cover Area

For the vegetation condition assessment of is used in practice, different vegetation indices, which may characterize the presence of a certain vegetation condition or vitality or vegetation health status. The image processing results are land surface temperature maps (Figure 15) and maps of the vegetation index (NDVI) (Figure 16). A comparison of Corine land cover (CLC) maps (for the period 2012–2018) showed changes in the spatial representation of individual classes of land cover (Table 4). There was a reduction in the area of mixed forest (313), and an increase in the area of non-irrigated arable land (211) and broad-leaved forest (311). The area of Transitional woodland-shrub (324) in 2018 was not identified. The current data for 2018 were selected for further processing.

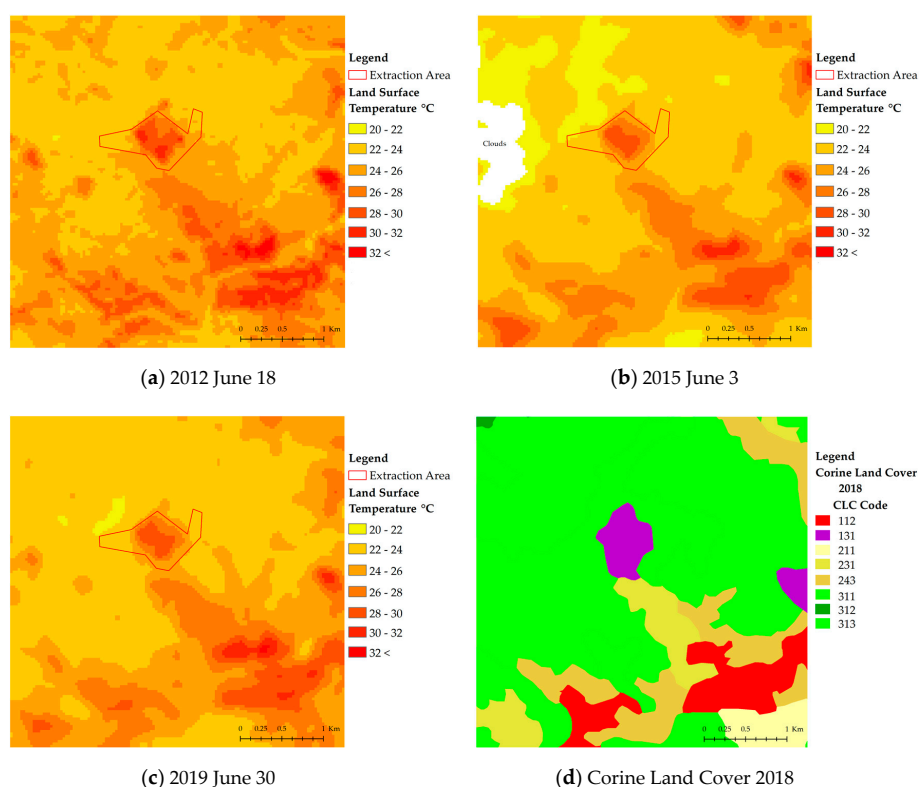


Figure 15. Land Surface Temperature of open-pit mine for years 2012 (a), 2015 (b), 2019 (c), and for Corine Land Cover (d).

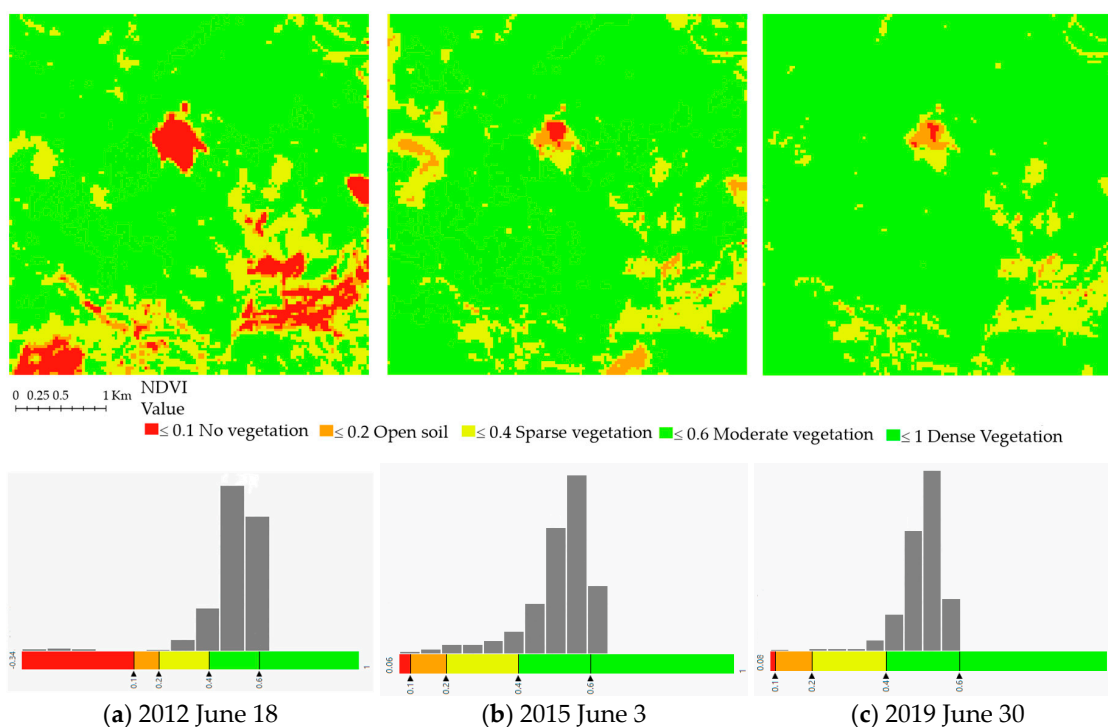


Figure 16. NDVI of open-pit mine for years 2012 (a), 2015 (b), 2019 (c).

Table 4. Representation of CLC classes for the reference period.

CLC Code	CLC			
	2012		2018	
	Area [ha]	Area [%]	Area [ha]	Area [%]
112 Discontinuous urban fabric	119.89	7.49	119.80	7.49
131 Mineral extraction sites	54.46	3.40	54.42	3.40
211 Non-irrigated arable land	19.74	1.23	47.24	2.95
231 Pastures	103.86	6.49	103.77	6.49
243 Land principally occupied by agriculture, with significant areas of natural vegetation	185.44	11.59	185.29	11.58
311 Broad-leaved forest	362.02	22.63	405.55	25.35
312 Coniferous forest	2.63	0.16	2.63	0.16
313 Mixed forest	709.38	44.35	681.30	42.58
324 Transitional woodland-shrub	42.58	2.66	0.00	0.00
Sum	1600.00	100	1600.00	100

Bold text presenting big changes in the values.

The analysis of the land surface temperature (for the years 2012, 2015, and 2019) showed that the course of the surface temperature copies the distribution of the Corine land cover. A comparison of Figures 13 and 15 shows that higher surface temperatures are in the areas affected by human activity, interpreted by ArcGIS 10.6.

In the surveyed locality are two parts where is surface mining realized (Figure 15d). The temperature in this locality which is comparable to the temperatures recorded in the city, even though the open-pit mine is located in the middle of a forested area. In June 2012, the temperature in the open-pit mine reached a value of 31 °C. In the second one locality (Margecany open-pit mine) temperature reached a value of 33.5 °C. The maximum observed temperature reached the level of 34.5 °C and was in the village of Jaklovce (Figure 15a). A similar temperature change in temperature has been observed in 2015 and 2019 (Figure 15b,c). In our study, it was also confirmed that differences in surface temperature arise similarly to how it is recognized in the work [38] due to differences in

the thermal capacity of buildings. The removal of vegetation and part of the soil cover due to mining (the open-pit mine did not expand during the observed period.) there was an increase in the incident thermal energy on the surface of the open-pit mine and this resulted in the more intense heating of the surface.

To assess the state of the environment, we chose the NDVI index like in the work [49]. The index takes its values from the interval $(-1, 1)$ which correlates with the content of green mass in the surface area represented by the pixel. Values corresponding to vegetation fall within the interval $(0.2 \text{ to } 0.9)$. Healthy and dense vegetation should befall within the interval $(0.6 \text{ to } 0.9)$. Figure 16 shows the result of the index calculation for 2012, 2015, and 2019, respectively. For the interpretation of obtained results was used an interface ArcGIS Pro. The lower part of Figure 16 shows the generated histograms, which present the theoretical frequencies of one side (left side) of the distribution of NDVI values. In all three histograms, the largest representation of frequencies is in the interval of 0.4 to 0.6. This interval has with incremental of years a growing tendency at decreasing frequencies of numbers of NDVI values in other intervals. These facts are verifiable in Table 5.

Table 5. Evaluation of NDVI index for the considered period.

Color	NDVI Index					
	2012		2015		2019	
	Area [ha]	Area [%]	Area [ha]	Area [%]	Area [ha]	Area [%]
	94.05	5.91	3.87	0.24	1.80	0.11
	44.10	2.77	28.26	1.78	11.52	0.72
	278.91	17.52	193.86	12.18	159.39	10.01
	1123.56	70.57	1216.71	76.43	1419.12	89.14
	51.39	3.23	149.31	9.38	0.18	0.01

Grey background presents the largest increase in values.

NDVI index is a simple vegetation index and is calculated through a normalized procedure. It is sensitive to green vegetation as well as areas covered by low vegetation [50]. The advantage of its use is also the possibility to derive it from images from the first Landsat satellite in 1972. NDVI index is used when comparing images at different periods to evaluate ecologically significant changes [51].

The spatial variability of the vegetation index NDVI with division according to (Earth Observing System) confirms the change in the condition of the represented vegetation in the selected area. By the comparison of orthophotos, no element was found of a significant decline of the forest by harvesting, for a general impact assessment of the open-pit mining processes and human activity is necessary to monitor the area in more detail.

4. Conclusions

At the state and public administration level it is necessary to deal with strategic planning and to include mining plans directly in the district structure plans of municipalities, regions, and the state. Mining plans at the national level help the industry to establish a stable planning framework for long-term mining. It is important to realize that existing mining sites may run out and therefore geological exploration is needed to further open up new sites. The results of the horizontal and vertical measurement of the current state of the open-pit mine only emphasize their applicability especially for:

- (1) Verification of the situation, if the mining at the present open-pit mine is provided under to legal provisions in force,
- (2) optimization of open-pit mining processes which could lead to increased safety and economy of the processes of surface mining,
- (3) identification and elimination of adverse impacts of the processes of surface mining to environmental,

- (4) settlement of possible legal disputes in the field of mineral resource extractions for the field real estate cadastre.

Digital maps, 3D models in Computer-Aided Design (CAD), and Geographical Information Systems (GIS) are an effective tool in strategic planning. They allow you to combine and overlap multiple levels of layers with different contents. In terms of the quality of the object's spatial position, the results from geodetic measurements (GNSS, TLS, RS, LIDAR, etc.) are considered as the most suitable.

The result of the processing and modeling of the measured data is the 3D model of the open-pit mine and its surroundings. The created 3D model is visualized using the colour scale of different parts of the open-pit mine. This model was created based on a sufficient amount of information obtained from direct measurements (satellite and terrestrial) and digitization of the previous mining map in analogue form. Aerial photogrammetry data were used to compare geodetic measurements.

The created model is a suitable basis for completing the mining process in the following years and monitoring the impact on the natural environment of the site.

After closed mining, it can be used as a basis for modeling the reclamation method, as the final shaping of landscaping must fulfil certain technical conditions:

- the angle of inclination of the newly formed solid shall be stable,
- safe drainage of surface water,
- preventing the area from drying out,
- separation of rock pieces from the walls of the open-pit mine must be controlled.

Surface mining disrupts the structure of the landscape. Aerial or satellite imagery is used to monitor changes in the country. Observations from Landsat 7 and 8 satellites were used to capture the potential impact of mining on the environment. Attention was focused on two factors, namely land surface temperature and vegetation condition. The results from temperature maps for the years 2012, 2015, and 2019 showed an increase in temperature in localities affected by human activity, either directly in the open-pit mine or in adjacent towns. The open-pit mine, despite being surrounded by forest, reached a temperature (2019—29.7 °C, 2015—29.3 °C, 2012—31 °C) comparable to the temperature in the town (2019—32 °C, 2015—32 °C, 2012—34.5 °C).

The results of the analysis of the NDVI index showed a change in the health status of vegetation in the area around the quarry. The values of the NDVI index in the range of 0.6 to 1, which represents healthy and dense vegetation, confirm the reduction of the area from 51.39 ha (2012) to 0.18 ha (2019). To evaluate the impact of mining on the health of vegetation, it is necessary to monitor the area in more detail. After adding data to the model of the wider environment, can be used as a basis for modeling the impact of mining on the change in the microclimate of the region.

Author Contributions: Conceptualization, S.L., M.B.G., and G.F.; methodology, S.L., M.B.G., and Z.K.; software, S.L.; validation, G.F., S.L., and M.B.G.; formal analysis, S.K.; investigation, Z.K.; resources, M.B.G., and Z.K.; data curation, S.L., and S.K.; writing—original draft preparation, S.L.; writing—review and editing, G.F.; visualization, S.L., and V.M.; supervision, V.M. All authors have read and agreed to the published version of the manuscript.

Funding: This research was funded by Scientific grant agency of Ministry of Education, science, research, and sport of the Slovak Republic, grant number VEGA 1/0754/18, VEGA 1/0600/20, VEGA 1/0403/18, KEGA 012TUKE-4/2019, KEGA 013TUKE-4/2019, SK-SRB-18-0053.

Conflicts of Interest: The authors declare no conflict of interest. The funders had no role in the design of the study; in the collection, analyses, or interpretation of data; in the writing of the manuscript, or in the decision to publish the results.

References

1. Lukáčová, K.; Badida, M.; Moravec, M.; Liptai, P. Particulate Matters Propagation by the Surface Winning. *Solid State Phenom.* **2015**, *244*, 197–202. [[CrossRef](#)]

2. Zvijáková, L.; Zelenakova, M.; Purcz, P. Evaluation of environmental impact assessment effectiveness in Slovakia. *Impact Assess. Proj. Apprais.* **2014**, *32*, 150–161. [[CrossRef](#)]
3. Wu, Z.; Lei, S.; Lu, Q.; Bian, Z.; Ge, S. Spatial distribution of the impact of surface mining on the landscape ecological health of semi-arid grasslands. *Ecol. Indic.* **2020**, *111*, 105996. [[CrossRef](#)]
4. Huang, X.; Sillanpää, M.; Gjessing, E.T.; Peräniemi, S.; Vogt, R.D. Environmental impact of mining activities on the surface water quality in Tibet: Gyama valley. *Sci. Total Environ.* **2010**, *408*, 4177–4184. [[CrossRef](#)]
5. Hendryx, M. The public health impacts of surface coal mining. *Extr. Ind. Soc.* **2015**, *2*, 820–826. [[CrossRef](#)]
6. Cianciolo, T.R.; McLaughlin, D.L.; Zipper, C.E.; Timpano, A.J.; Soucek, D.J.; Schoenholtz, S.H. Impacts to water quality and biota persist in mining-influenced Appalachian streams. *Sci. Total Environ.* **2020**, *717*, 137216. [[CrossRef](#)]
7. Ranjan, R. Assessing the impact of mining on deforestation in India. *Resour. Policy* **2019**, *60*, 23–35. [[CrossRef](#)]
8. Kahhat, R.; Parodi, E.; Larrea-Gallegos, G.; Mesta, C.; Vázquez-Rowe, I. Environmental impacts of the life cycle of alluvial gold mining in the Peruvian Amazon rainforest. *Sci. Total Environ.* **2019**, *662*, 940–951. [[CrossRef](#)]
9. Werner, T.T.; Bebbington, A.; Gregory, G. Assessing impacts of mining: Recent contributions from GIS and remote sensing. *Extr. Ind. Soc.* **2019**, *6*, 993–1012. [[CrossRef](#)]
10. Krümmelbein, J.; Horn, R.; Raab, T.; Bens, O.; Hüttl, R.F. Soil physical parameters of a recently established agricultural recultivation site after brown coal mining in Eastern Germany. *Soil Tillage Res.* **2010**, *111*, 19–25. [[CrossRef](#)]
11. Moomen, A.-W.; Bertolotto, M.; Lacroix, P.; Jensen, D. Inadequate adaptation of geospatial information for sustainable mining towards agenda 2030 sustainable development goals. *J. Clean. Prod.* **2019**, *238*, 117954. [[CrossRef](#)]
12. Labant, S.; Stančková, H.; Weiss, R. Geodetic Determining of Stockpile Volume of Mineral Excavated in Open Pit Mine. *Geosci. Eng.* **2013**, *59*, 30–40. [[CrossRef](#)]
13. Vrublová, D.; Kapica, R.; Gibesová, B.; Mudrun'ka, J.; Strus', A. Application of GNSS technology in surface mining. *Geod. Cartogr.* **2016**, *42*, 122–128. [[CrossRef](#)]
14. Gao, J.X.; Hu, H. Advanced GNSS technology of mining deformation monitoring. *Procedia Earth Planet. Sci.* **2009**, *1*, 1081–1088.
15. Xu, H. Extraction of Urban Built-up Land Features from Landsat Imagery Using a Thematic-oriented Index Combination Technique. *Photogramm. Eng. Remote Sens.* **2007**, *73*, 1381–1391. [[CrossRef](#)]
16. Deliormanli, A.; Norbert, M.; Otoo, J. Using terrestrial 3D laser scanning and optical methods to determine orientations of discontinuities at a granite quarry. *Int. J. Rock Mech. Min. Sci.* **2014**, *66*, 41–48. [[CrossRef](#)]
17. Gama, F.; Cantone, A.; Mura, J.; Pasquali, P.; Paradella, W.; Ribeiro, A.; Silva, G. Monitoring subsidence of open pit iron mines at Carajás Province based on SBAS interferometric technique using TerraSAR-X data. *Remote Sens. Appl. Soc. Environ.* **2017**, *8*, 199–211. [[CrossRef](#)]
18. Wang, J.; Wang, L.; Jia, M.T.; He, Z.; Bi, L. Construction and Optimization Method of the Open-pit Mine DEM Based on the Oblique Photogrammetry Generated DSM. *Measurement* **2019**, *152*, 107322. [[CrossRef](#)]
19. Agüera-Vega, F.; Carvajal-Ramírez, F.; Martínez-Carricondo, P. Assessment of Photogrammetric Mapping Accuracy Based on Variation Ground Control Points Number Using Unmanned Aerial Vehicle. *Measurement* **2016**, *98*, 221–227. [[CrossRef](#)]
20. Niethammer, U.; James, M.; Rothmund, S.; Travelletti, J.; Joswig, M. UAV-based remote sensing of the Super-Sauze landslide: Evaluation and results. *Eng. Geol.* **2012**, *128*, 2–11. [[CrossRef](#)]
21. Stanek, V.; Hostinová, G.; Kopacik, A. *Geodesy in Construction*; Jaga Group: Bratislava, Slovakia, 2007.
22. Rakay, S.; Zuzik, J.; Weiss, G.; Labant, S. Surveying of inaccessible rock faces and volume calculation of the irregular solids using robotic total station. *Acta Montan. Slovaca* **2013**, *18*, 164–171.
23. Long, N.Q.; Buczek, M.M.; Hien, L.P.; Szlapin'ska, S.A.; Nam, B.X.; Nghia, N.V.; Cuong, C.X. Accuracy assessment of mine walls' surface models derived from terrestrial laser scanning. *Int. J. Coal Sci. Technol.* **2018**, *5*, 328–338. [[CrossRef](#)]
24. Armstrong, B.; Blackwood, A.; Penzokajewski, P.; Menter, C.; Herries, A. Terrestrial laser scanning and photogrammetry techniques for documenting fossil-bearing palaeokarst with an example from the Drimolen Palaeocave System, South Africa. *Archaeol. Prospect.* **2017**, *25*, 45–58. [[CrossRef](#)]
25. Schmitz, B.; Holst, C.; Medic, T.; Lichti, D.; Kuhlmann, H. How to Efficiently Determine the Range Precision of 3D Terrestrial Laser Scanners. *Sensors* **2019**, *19*, 1466. [[CrossRef](#)]

26. Shahbazi, M.; Sohn, G.; Théau, J.; Menard, P. Development and Evaluation of a UAV-Photogrammetry System for Precise 3D Environmental Modeling. *Sensors* **2015**, *15*, 27493–27524. [[CrossRef](#)]
27. Ali-Sisto, D.; Gopalakrishnan, R.; Kukkonen, M.; Savolainen, P.; Packalen, P. A method for vertical adjustment of digital aerial photogrammetry data by using a high-quality digital terrain model. *Int. J. Appl. Earth Obs. Geoinf.* **2020**, *84*, 101954. [[CrossRef](#)]
28. Keawaram, B.; Dumrongchai, P. Comparisons of Surveying with Terrestrial Laser Scanner and Total Station for Volume Determination of Overburden and Coal Excavations in Large Open-Pit Mine. *Int. J. Geol. Environ. Eng.* **2017**, *11*, 1031–1039.
29. Tong, X.; Liu, X.; Chen, P.; Liu, S.; Luan, K.; Li, L.; Liu, S.; Liu, X.; Xie, H.; Jin, Y.; et al. Integration of UAV-Based Photogrammetry and Terrestrial Laser Scanning for the Three-Dimensional Mapping and Monitoring of Open-Pit Mine Areas. *Remote Sens.* **2015**, *7*, 6635–6662. [[CrossRef](#)]
30. Nunoo, S.; Tannant, D.D.; Newcomen, H.W. Slope monitoring practices at open pit porphyry mines in British Columbia, Canada. *Int. J. Min. Reclam. Environ.* **2016**, *30*, 245–256. [[CrossRef](#)]
31. Xu, Z.; Xu, E.; Wu, L.; Liu, S.; Mao, Y. Registration of Terrestrial Laser Scanning Surveys Using Terrain-Invariant Regions for Measuring Exploitative Volumes over Open-Pit Mines. *Remote Sens.* **2019**, *11*, 606. [[CrossRef](#)]
32. Wajs, J. Research on surveying technology applied for DTM modelling and volume computation in open pit mines. *Min. Sci.* **2016**, *22*, 75–83.
33. Correia Neto, J.; Mariz, J.; de Souza, J.; Vasconcelos, S.; Rocha, S. Elaboration of planimetric model of open pit with multiple benches through the conventional methodology and the use of unmanned aerial vehicles (UAV). *Tecnologia em Metalurgia, Materiais e Mineração* **2020**, *16*, 439–446. [[CrossRef](#)]
34. Török, Á.; Bögöly, G.; Somogyi, A.; Lovas, T. Application of UAV in Topographic Modelling and Structural Geological Mapping of Quarries and Their Surroundings—Delineation of Fault-Bordered Raw Material Reserves. *Sensors* **2020**, *20*, 489. [[CrossRef](#)]
35. Tucci, G.; Gebbia, A.; Conti, A.; Fiorini, L.; Lubello, C. Monitoring and Computation of the Volumes of Stockpiles of Bulk Material by Means of UAV Photogrammetric Surveying. *Remote Sens.* **2019**, *11*, 1471. [[CrossRef](#)]
36. Drabiková, E.; Svetlík, J. Improving management of the company through Cranfield process model. *MM Sci. J.* **2018**, 2153–2157. [[CrossRef](#)]
37. Baláž, P.; Kúšik, D. Nerastné Suroviny Slovenskej Republiky 2015 (Stav 2014). In *Slovak Minerals Yearbook 2015 (State 2014)*; State Geological Institute of Dionyz Stur: Bratislava, Slovakia, 2015.
38. Fawzi, N.I.; Jatmiko, R. Heat Island Detection in Coal Mining Areas Using Multitemporal Remote Sensing. In *Proceedings of the 36th Asian Conference on Remote Sensing, Metro Manila, Philippines, 24–28 October 2015*; pp. 1–9.
39. Sun, W.; Zhang, H.; Cao, Y.; Zhang, X.; Ji, X.; Li, F. Monitoring the ecological environment of open-pit coalfields in cold zones of Northeast China using Landsat time series images of 2000–2015. *Tehnicki Vjesnik/Technical Gazette* **2017**, *24*, 129–140.
40. Wang, S.; Huang, J.; Yu, H.; Ji, C. Recognition of Landscape Key Areas in a Coal Mine Area of a Semi-Arid Steppe in China: A Case Study of Yimin Open-Pit Coal Mine. *Sustainability* **2020**, *12*, 2239. [[CrossRef](#)]
41. *Landsat 8 (L8) Science Data Users Handbook Version 2*; Department of the Interior U.S. Geological Survey: Washington, DC, USA, 2016.
42. *Landsat 7 (L7) Science Data Users Handbook Version 2*; Department of the Interior U.S. Geological Survey: Washington, DC, USA, 2019.
43. Avdan, U.; Jovanovska, G. Algorithm for automated mapping of land surface temperature using Landsat 8 satellite data. *J. Sens.* **2016**, *2016*, 1–8. [[CrossRef](#)]
44. Kuzevič'ová, Ž.; Gergel'ová, M.; Kuzevič', Š.; Palková, J. Spatial interpolation and calculation of the volume an irregular solid. *Int. J. Eng. Appl. Sci.* **2014**, *4*, 14–21.
45. Klimánek, M. *Digitální Modely Terénu*; Mendelova Zemědělská a Lesnická Univerzita: Brno, Czech Republic, 2006; ISBN 80-7157-982-3.
46. Passalacqua, P.; Hillier, J. Innovative analysis and use of high resolution DTMs for understanding Earth-surface processes. *Earth Surf. Process. Landf.* **2014**, *39*, 1400–1403. [[CrossRef](#)]
47. Menegaki, M.E.; Kaliampakos, D.C. Evaluating mining landscape: A step forward. *Ecol. Eng.* **2012**, *43*, 26–33. [[CrossRef](#)]

48. Wycisk, P.; Hubert, T.; Gossel, W.; Neumann, C. High-resolution 3D spatial modelling of complex geological structures for an environmental risk assessment of abundant mining and industrial megasites. *Comput. Geosci.* **2009**, *35*, 165–182. [[CrossRef](#)]
49. Bharath, S.; Rajan, K.S.; Ramachandra, T.V. Land surface temperature responses to land use land cover dynamics. *Geoinfor. Geostat. Overv.* **2013**, *54*, 50–78.
50. Xue, J.; Su, B. Significant remote sensing vegetation indices: A review of developments and applications. *J. Sens.* **2017**, *2017*, 1–17. [[CrossRef](#)]
51. Saini, V.; Gupta, R.P.; Arora, M.K. Chapter 17—Environmental Monitoring in the Jharia Coalfield, India: Vegetation Indices and Surface Temperature Measurements. In *Coal and Peat Fires: A Global Perspective*; Elsevier: Amsterdam, The Netherlands, 2019; pp. 359–385. ISBN 978-0-12-849885-9.



© 2020 by the authors. Licensee MDPI, Basel, Switzerland. This article is an open access article distributed under the terms and conditions of the Creative Commons Attribution (CC BY) license (<http://creativecommons.org/licenses/by/4.0/>).